Synthetic and Structural Investigations of Organomagnesium Complexes of Hybrid Boraamidinate/Amidinate Ligands and Their Use in the Polymerization of *rac*-Lactide

Tristram Chivers,* Chantall Fedorchuk, and Masood Parvez

Department of Chemistry, University of Calgary, Calgary, Alberta, Canada T2N 1N4

Received September 22, 2004

The complexation chemistry of the protio and lithium bamam complexes (H)bamam-**1** and (Li)bamam-**1** [bamam-**1** = {DippN(Ph)B(N^{t}Bu)C^{n}Bu(N^{t}Bu)}, Dipp = 2,6-diisopropylphenyl] with magnesium is explored. Emphasis is placed on the preparation and characterization of both solvated and unsolvated aryl/alkylmagnesium bamam complexes (RMgL)bamam-**1** (**1**, R = ^{t}Bu, L = none; **2**, R = Mes, L = none; **3**, R = Me, L = OEt$_2$; **4**, R = Ph, L = THF; **5**, R = ^{i}Pr, L = THF; **6**, R = ^{n}Bu, L = OEt$_2$). X-ray structural analyses reveal that the Mg bamam-**1** complexes are six-membered rings, which adopt a distorted boat structure as a result of a transannular Mg−N interaction (2.39−2.85 Å). Variable-temperature NMR spectra indicate this interaction is maintained in solution. Preliminary studies of the polymerization of *rac*-lactide with complexes **3**−**6** revealed that **3** and **4** promote the polymerization process producing hetero-biased polylactide, whereas **5** and **6** are inactive.

Introduction

The chemistry of β-diketiminate (nacnac) **A** (Chart 1) metal complexes is of substantial current interest.[1] β-Diketiminates have been recognized as useful monoanionic spectator ligands due to their strong binding to metal centers and tunability by variation of the backbone substituents. However, less emphasis has been placed on examining the effect of altering the backbone of the ligand **A**. Recently we reported our efforts to generate hybrid boraamidinate/amidinate (bamam) ligands **B** (Chart 1) that are formally isoelectronic with the ligands **A**.[2] In particular, it was of interest to assess the influence of the replacement of an R′CCR″ unit in **A** by the polar, isoelectronic R′NBR″ unit in **B**. In contrast to protio nacnac complexes, which adopt an acyclic structure, cf., **A** (Chart 1),[1] the presence of the electron-accepting boron atom in the bamam backbone can promote the formation of four-membered BNCN rings in protio complexes (**C**).[2]

Herein, we report the synthesis and structural characterization of a series of magnesium bamam complexes. In view of the recent interest in the application of the related Mg-based β-diketiminates as catalysts for the ring-opening polymerization (ROP) of lactide (LA)-producing polylactide (PLA),[3−7] we have also carried out preliminary investigations of the use of the magnesium bamam complexes as initiators for this polymerization process.

Chart 1

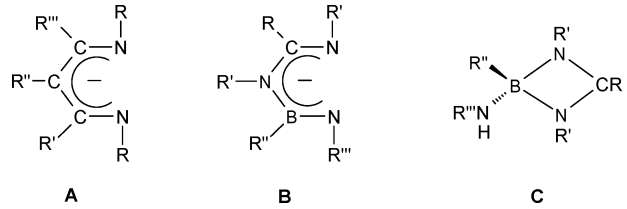

Results and Discussion

Syntheses and X-ray Structures of (RMgL)-bamam-1 Complexes. We recently reported the preparation and characterization of protio bamam derivatives, in which either four-membered BNCN rings with an exocyclic amido (NHR) substituent (H)bamam-**1**,**2** (Chart 2) or acyclic NBNCN chelating ligands (H)bamam-**3**,**4** (Chart 2) are formed depending on the substituents attached to the nitrogen or carbon atoms.[2] Monolithiation of the exocyclic amido substituent on the ring system in (H)bamam-**1** provides the alkali derivative (Li)bamam-**1** (Chart 2).[2] The protio and lithium derivatives [(H)bamam-**1** and (Li)bamam-**1**] serve as precursors to magnesium bamam complexes (RMgL)bamam-**1**, as indicated below.

The treatment of (Li)bamam-**1** with the appropriate Grignard reagent in toluene affords either unsolvated aryl/alkylmagnesium complexes (**1** and **2**) or solvated

* To whom correspondence should be addressed. Tel: (403) 220-5741. Fax: (403) 289-9488. E-mail: chivers@ucalgary.ca.

(1) For a review, see: Bourget-Merle, L.; Lappert, M. F.; Severn, J. R. *Chem. Rev*. **2002**, *102*, 3031.

(2) Chivers, T.; Fedorchuk, C.; Parvez, M. *Inorg. Chem*. **2004**, *43*, 2643.

(3) Chisholm, M. H.; Phomphrai, K. *Inorg. Chim. Acta*. **2003**, *350*, 121, and references therein.

(4) Chamberlain, B. M.; Cheng, M.; Moore, D. R.; Ovitt, T. M.; Lobkovsky, E. B.; Coates, G. W. *J. Am. Chem. Soc*. **2001**, *123*, 3229.

(5) Chisholm, M. H.; Huffman, J. C.; Phomphrai, K. *J. Chem. Soc., Dalton Trans*. **2001**, 222.

(6) Chisholm, M. H.; Gallucci, J.; Phomphrai, K. *Inorg. Chem*. **2002**, *41*, 2785.

(7) Dove, A. P.; Gibson, V. C.; Marshall, E. L.; White, A. J. P.; Williams, D. J. *Dalton Trans.* **2004**, 570.

10.1021/om049263i CCC: $30.25
Publication on Web 01/11/2005

Chart 2

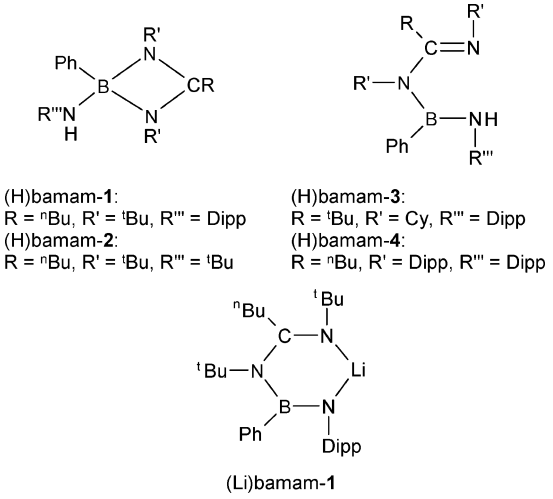

Scheme 1

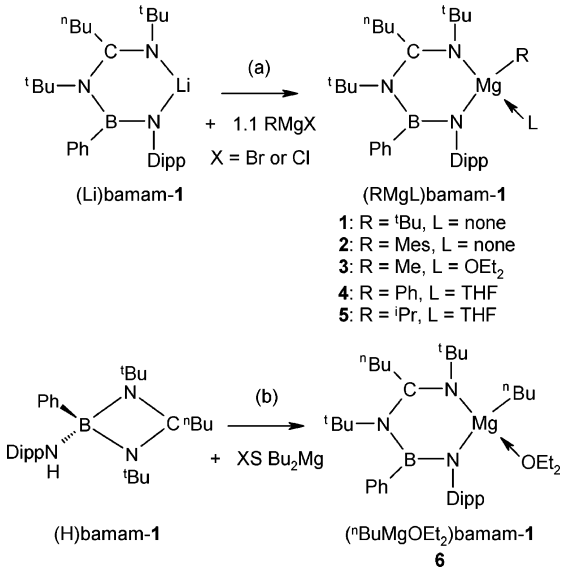

aryl/alkylmagnesium complexes (**3**−**5**) in 58−79% yields (Scheme 1a). The reaction of (H)bamam-**1** with $^{n/s}Bu_2Mg$ results in the formation of the diethyl ether-solvated *n*-butylmagnesium complex **6** (Scheme 1b) in 60% yield. The magnesium complexes **1**−**6** were characterized by CHN analyses, multinuclear (^1H, ^{11}B, ^{13}C) NMR spectroscopy, and single-crystal X-ray structural determinations. The molecular geometry and atomic numbering scheme for the complexes **1**−**6** are shown in Figures 1 and 2, and pertinent structural parameters are summarized in Tables 1 and 2.

A variety of ligand-to-metal bonding modes including terminal, bridging, or *N*,*N*′-chelation has been reported for metal complexes of *β*-diketiminates.[1] Magnesium nacnac complexes employing bulky aryl[4−18] or silyl[19] substituents on the nitrogen atoms usually adopt the

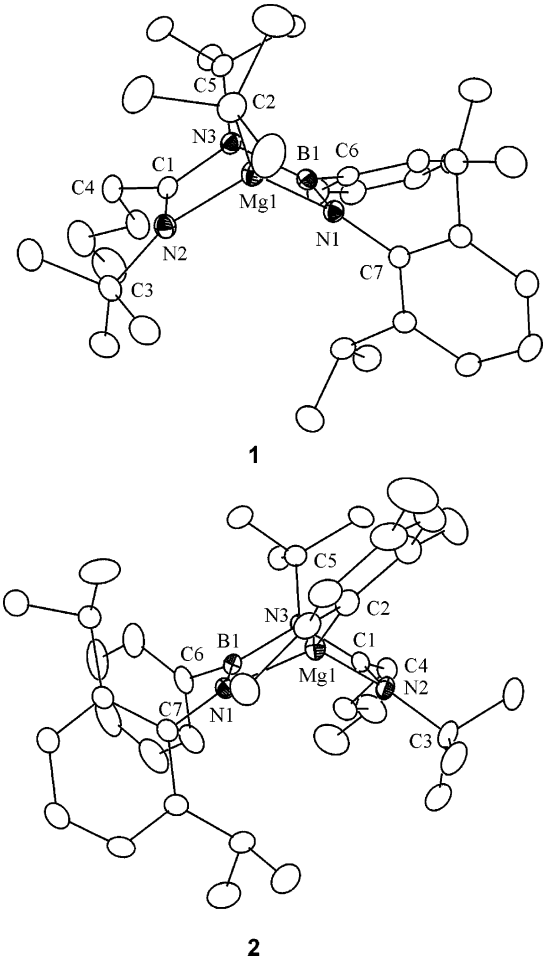

Figure 1. Thermal ellipsoid plots (side views) of the unsolvated complexes **1** and **2**.

N,*N*′-coordination mode. Recently, however, Winter et al. have reported *π*-bonding to the nacnac ligand in the organomagnesium complex CpMg{CH[(CMe)N^{t}Bu]$_2$}.[20] In *N*,*N*′-chelated complexes, the metallacycle is usually planar, although distortions toward a boat structure have been observed.[1] In contrast, the bamam ligand in **1** folds significantly in the solid state (Figure 1). The six-membered ring formed from the backbone of the bamam ligand and the metal center can be described as a distorted boat structure in which the Mg(1) and N(3) atoms lie 0.606 and 0.577 Å above the least-squares plane formed by B(1), N(1), N(2), and C(1). The related *β*-diketiminate complex (MeMgTHF)BDI-**1** (BDI-**1** = {CH[(CMe)NDipp]$_2$}) also adopts a boat conformation similar to that observed for **1**; however, the distortion

(8) Bailey, P. J.; Dick, C. M. E.; Fabre, S.; Parsons, S. *J. Chem. Soc., Dalton Trans.* **2000**, 1655.
(9) Gibson, V. C.; Segal, J. A.; White, A. J. P.; Williams, D. J. *J. Am. Chem. Soc.* **2000**, *122*, 7120.
(10) Bailey, P. J.; Liddle, S. T.; Morrison, C. A.; Parsons, S. *Angew. Chem., Int. Ed.* **2001**, *40*, 4463.
(11) Bailey, P. J.; Coxall, R. A.; Dick, C. M. E.; Fabre, S.; Parsons, S. *Organometallics* **2001**, *20*, 798.
(12) Prust, J.; Most, K.; Müller, I.; Alexopoulos, E.; Stasch, A.; Usón, I.; Roesky, H. W. *Z. Anorg. Allg. Chem.* **2001**, *627*, 2032.
(13) Dove, A. P.; Gibson, V. C.; Marshall, E. L.; White, A. J. P.; Williams, D. J. *Chem. Commun.* **2002**, 1208.
(14) Hao, H.; Roesky, H. W.; Ding, Y.; Cui, C.; Schormann, M.; Schmidt, H.-G.; Noltemeyer, M.; Zemva, B. *J. Fluor. Chem.* **2002**, *115*, 143.
(15) Harder, S. *Organometallics* **2002**, *21*, 3782.
(16) Bailey, P. J.; Coxall, R. A.; Dick, C. A.; Fabre, S.; Henderson, L. C.; Herber, C.; Liddle, S. T.; Loroño-González, D.; Parkin, A.; Parsons, S. *Chem. Eur. J.* **2003**, *9*, 4280.
(17) Dove, A. P.; Gibson, V. C.; Hormnirun, P.; Marshall, E. L.; Segal, J. A.; White, A. J. P.; Williams, D. J. *Dalton Trans.* **2003**, 3088.
(18) Kennedy, A. R.; Mair, F. S. *Acta Crystallogr. Sect. C: Cryst. Struct. Commun.* **2003**, *59*, M549.
(19) Caro, C. F.; Hitchcock, P. B.; Lappert, M. F. *Chem. Commun.* **1999**, 1433.
(20) El-Kaderi, H. M.; Xia, A.; Heeg, M. J.; Winter, C. H. *Organometallics* **2004**, *23*, 3488.

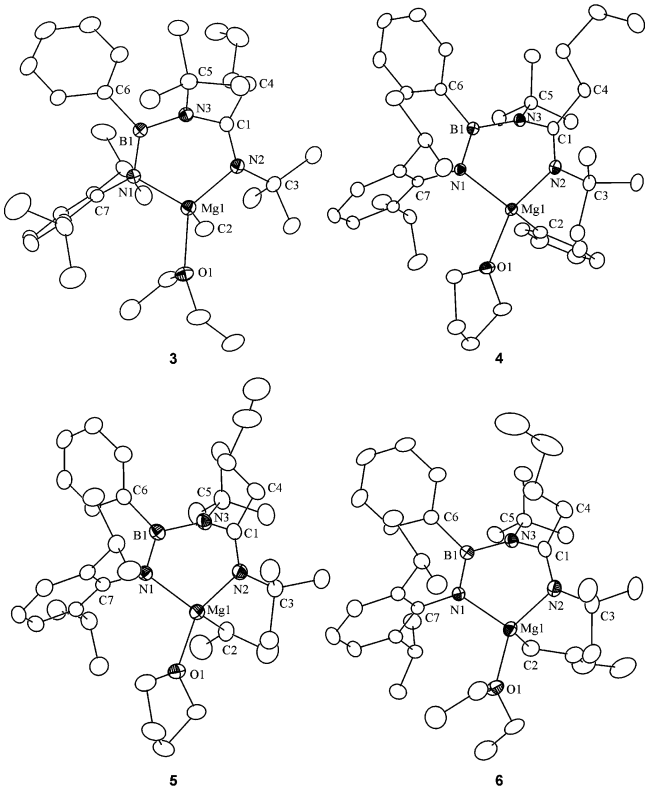

Figure 2. Thermal ellipsoid plots (top views) of the solvated complexes **3**−**6**.

is substantially smaller, with the magnesium and central carbon C(3) atoms lying 0.126 and 0.268 Å above the least-squares plane.[8]

For *N*,*N*′-chelated *β*-diketiminate complexes, the change in bonding mode from a planar ligand conformation to a boat form is caused by steric crowding around the metal center.[1] In contrast, there is substantial interaction between the central nitrogen atom of the ligand and the metal center in **1** and **2** (*d*[Mg(1)−N(3)] = 2.39 Å, Table 1), cf., sum of van der Waals radii of magnesium and nitrogen (3.28 Å).[21] The Mg(1)−N(3) distance is greater than typical Mg−N single bond lengths, e.g., 2.052(2)−2.065(2) Å in the tetrahedral complex Mg{CH[(CMe)N^{i}Pr]$_2$},[20] but is similar to the value of 2.350(3) Å observed for the Mg−N dative bond in Li[(TMEDA)Mg(C≡CPh)$_3$] (TMEDA = [Me$_2$NCH$_2$]$_2$).[22] This Mg(1)−N(3) transannular interaction in **1** and **2** results in the pronounced folding of the six-membered ring.

Inspection of the bond distances in **1** and **2** (Table 1) indicates localized *π*-bonding within the backbone of the bamam ligand. The B(1)−N(1) bond lengths of 1.36−1.37 Å and the B(1)−N(3) distance of 1.56−1.57 Å reflect double and single bonds, respectively.[23] Concomitantly, the C(1)−N(2) bond lengths of 1.28−1.29 Å and the C(1)−N(3) distances of 1.43−1.44 Å are typical double and single bond values, respectively. The geometry of N(3) is trigonal planar, with each of the bond angles very close to 120° (Table 2). There is substantial variation in the bond angles around the remaining atoms as a result of the folding of the six-membered ring, although in each case the sum of the angles is near 360°, indicating a distorted trigonal planar geometry for these atoms. The endocyclic bond angles at N(1) and N(2) are ca. 99° and ca. 101°, respectively, while the endocyclic bond angles at B(1) and C(1) are both ca. 114°. The bond angles around the three-coordinate magnesium center are in the ranges 95−143° for **1** and 99−134° for **2**. The larger distortion in the former case presumably reflects the influence of the more bulky *tert*-butyl group. There is a small disparity of ca. 0.08 Å in the Mg−N distances in both complexes, implying a dative coordinate bond for the longer Mg(1)−N(2) interaction. Taken together, these metrical parameters are consistent with a structure involving localized *π*-bonding (**D**, Chart 3) in contrast to the *β*-diketiminate ligand, which is usually *π*-delocalized (**A**, Chart 1). The folding of the six-membered ring brings the p-orbital on N(3) into a suitable orientation to facilitate lone-pair donation to the magnesium center.

The remaining complexes **3**−**6** also assume a folded structure in the solid state (Figure 2), albeit with a significantly weaker transannular Mg−N interaction (range 2.68−2.85 Å, Table 1) as a result of the solvation of the magnesium center by a solvent molecule. Excluding the weak cross-ring interaction, the geometry around Mg is distorted tetrahedral with bond angles in the range ca. 93−132°, the most acute angle being associated with the bite of the chelating bamam ligand [N(1)−Mg(1)−N(2), Table 2]. The disparity of ca. 0.10 Å in the Mg−N bond lengths in these solvated complexes is slightly more pronounced than that observed for **1** and **2**. Perusal of the structural parameters in Table 1 reveals an interesting trend involving the Mg(1)−N(3) and N(3)−B(1) bond distances. The stronger Mg−N interaction in **1** and **2** is associated with weaker B(1)−N(3) bonds (1.56−1.57 Å), cf. 1.50−1.52 Å in **3**−**6**. The other bond distances in the backbone of the bamam-**1**

Table 1. Selected Bond Distances (Å) for Complexes 1−6

	1	2	3	4	5	6
Mg(1)−N(1)	2.004(2)	2.017(2)	2.059(1)	2.034(1)	2.041(2)	2.049(2)
Mg(1)−N(2)	2.080(2)	2.101(2)	2.155(2)	2.137(1)	2.148(2)	2.155(2)
Mg(1)−N(3)	2.390(2)	2.389(2)	2.683(1)	2.845(1)	2.849(1)	2.843(2)
Mg(1)−O(1)			2.143(1)	2.111(1)	2.114(2)	2.145(2)
Mg(1)−C(2)	2.157(3)	2.129(3)	2.174(2)	2.159(2)	2.185(3)	2.155(2)
N(1)−C(7)	1.423(3)	1.431(3)	1.412(2)	1.413(2)	1.413(3)	1.417(2)
N(2)−C(1)	1.287(3)	1.282(3)	1.288(2)	1.295(2)	1.284(3)	1.284(3)
N(2)−C(3)	1.487(4)	1.501(3)	1.496(2)	1.502(2)	1.506(3)	1.512(3)
N(3)−B(1)	1.563(4)	1.568(3)	1.514(2)	1.522(2)	1.509(4)	1.503(3)
N(3)−C(1)	1.431(3)	1.435(3)	1.422(2)	1.412(2)	1.422(4)	1.426(3)
N(3)−C(5)	1.517(3)	1.521(3)	1.517(2)	1.514(2)	1.519(4)	1.519(2)
B(1)−N(1)	1.374(3)	1.362(4)	1.384(2)	1.378(2)	1.389(4)	1.388(3)
B(1)−C(6)	1.597(4)	1.595(4)	1.596(2)	1.598(2)	1.597(4)	1.613(3)
C(1)−C(4)	1.515(4)	1.513(4)	1.516(2)	1.523(2)	1.511(4)	1.511(3)

Table 2. Selected Bond Angles (deg) for Complexes 1−6

	1	2	3	4	5	6
N(2)−Mg(1)−O(1)			111.45(5)	121.13(5)	114.9(9)	114.02(7)
N(2)−Mg(1)−N(1)	95.43(9)	99.47(9)	94.03(5)	93.12(5)	92.99(9)	93.22(7)
N(2)−Mg(1)−C(2)	121.1(1)	124.2(1)	117.47(7)	110.80(6)	112.4(1)	114.92(9)
N(1)−Mg(1)−C(2)	143.0(1)	133.7(1)	132.38(6)	131.69(6)	130.9(1)	131.44(9)
N(1)−Mg(1)−O(1)			100.97(5)	100.78(5)	101.83(9)	99.23(7)
C(2)−Mg(1)−O(1)			99.32(6)	101.26(5)	104.0(1)	103.45(9)
B(1)−N(1)−Mg(1)	98.3(2)	99.6(2)	104.4(1)	109.2(9)	107.9(2)	108.3(1)
B(1)−N(1)−C(7)	126.8(2)	127.2(2)	126.1(1)	124.8(1)	124.0(2)	122.8(2)
C(7)−N(1)−Mg(1)	134.9(2)	133.2(2)	129.3(1)	126.0(9)	128.2(2)	128.6(1)
Mg(1)−N(2)−C(3)	128.5(2)	132.1(2)	124.9(1)	123.32(9)	125.2(2)	125.0(1)
Mg(1)−N(2)−C(1)	100.1(2)	101.3(2)	107.3(1)	111.44(9)	111.1(1)	110.8(1)
C(1)−N(2)−C(3)	128.5(2)	126.6(2)	127.8(1)	124.9(1)	123.7(2)	124.1(2)
C(1)−N(3)−B(1)	119.6(2)	118.0(2)	120.4(1)	122.0(1)	121.7(2)	120.8(2)
C(1)−N(3)−C(5)	119.6(2)	118.5(2)	118.2(1)	118.8(1)	116.2(2)	116.7(2)
C(5)−N(3)−B(1)	119.7(2)	119.3(2)	120.9(1)	119.3(1)	122.1(2)	122.5(2)
N(3)−B(1)−N(1)	114.6(2)	113.5(2)	117.2(1)	118.8(1)	118.5(3)	118.0(2)
N(3)−B(1)−C(6)	120.6(2)	121.3(2)	118.4(1)	117.7(1)	119.2(2)	118.9(2)
C(6)−B(1)−N(1)	124.7(3)	125.1(2)	124.4(2)	123.5(1)	122.3(2)	123.1(2)
N(2)−C(1)−C(4)	125.2(3)	127.0(2)	127.9(2)	125.2(1)	125.7(3)	126.0(2)
N(2)−C(1)−N(3)	114.2(2)	113.5(2)	116.5(1)	117.7(1)	119.0(2)	118.8(2)
N(3)−C(1)−C(4)	120.6(2)	119.5(2)	115.3(1)	117.1(1)	115.2(2)	115.1(2)

Table 3. Polymerization of *rac*-Lactide[a]

initiator	active	solvent	time (h)	conversion[b] (%)	M_w/M_n[c]	tacticity[d]	M_n, g mol^{-1} ($\times 10^3$)	Mg(1)−N(3) (Å)
3	yes	$CDCl_3$	2.5	61	1.44	hetero-biased	61.1	2.683(1)
4	yes	$CDCl_3$	2	100	1.74	atactic		2.845(1)
5	no	$CDCl_3$						2.849(1)
6	no	$CDCl_3$						2.843(2)

[a] [*rac*-LA]:[initiator] = 100. [b] Determined by ^{1}H NMR spectroscopy. [c] Average determined by size-exclusion chromatography measurements. [d] Determined by homonuclear decoupled ^{1}H NMR spectroscopy.

Chart 3

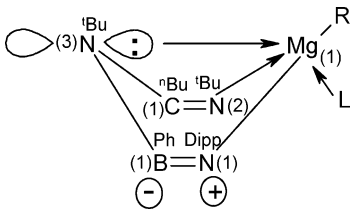

D

ligand exhibit a much smaller variation across the series **1**−**6**. The stronger transannular interaction in **1** and **2** also results in significantly smaller endocyclic bond angles at B(1) and C(1).

The ^{1}H NMR spectra of complexes **1**−**6** indicate that the asymmetry present in the solid-state structures is maintained in solution. For example, two separate methine signals and four doublets of equal intensity are observed for the ^{i}Pr methyl groups of the Dipp substituent. This reflects the low symmetry inherent in the out-of-plane bonding mode observed in the solid-state structures, as well as indicating that there is hindered rotation of the N-Dipp group in solution most likely due to the steric properties of this ligand. The ^{1}H NMR spectra of the complexes **1**−**6** are essentially unaltered over the temperature range −60 to +100 °C, suggesting that the transannular Mg(1)−N(3) interaction is maintained in solution. By comparison, the variable-temperature ^{1}H NMR spectra for the sterically similar β-diketiminate scandium complex $(Me_3SiCH_2)_2Sc\{CH[(C^t$-Bu)NDipp$]_2\}$, which has no transannular interaction, provide evidence for an equilibration of two equivalent out-of-plane structures via an in-plane transition state.[24] Apparently the Mg−N interaction prevents this process from occurring in complexes **1**−**6**. The ^{11}B NMR spectra of complexes **1**−**6** exhibit broad resonances at ca. 32−34 ppm, indicative of a three-coordinate boron environment in each case.[25]

Preliminary Investigations of the Polymerization of *rac*-Lactide. The recent interest in the application of Mg-based β-diketiminates as catalysts for the polymerization of *rac*-lactide to polylactide[3−7] prompted a preliminary investigation of the behavior of organomagnesium bamam-**1** complexes as polymerization initiators. The polymerization was studied for complexes **3**−**6**. As indicated in Table 3, complexes **3** and **4** were found to be active, whereas **5** and **6** are inactive. Since the transannular Mg−N distances in **4**, **5**, and **6** are equal (see Table 3), the activity of these complexes is apparently not directly related to the strength of this interaction.

Complex **3** promotes polymerization when the process is carried out in $CDCl_3$, affording 61% conversion within 2.5 h. Determination of the stereochemical microstructure of the resulting PLA was achieved through inspection of the methine region of the homonuclear decoupled ^{1}H NMR spectra of the polymers. It has been determined from Bernoullian statistics that atactic PLA exhibits five resonances in its spectrum, while perfectly heterotactic PLA shows only two resonances.[26] When

(21) Bondi, A. *J. Phys. Chem.* **1964**, *68*, 441.
(22) Schubert, B.; Weiss, E. *Chem. Ber.* **1984**, *117*, 366.
(23) Paetzold, P. *Phosphorus, Sulfur, Silicon*. **1994**, *93*−*94*, 39.
(24) Hayes, P. G.; Piers, W. E.; Lee, L. W. M.; Knight, L. K.; Parvez, M.; Elsegood, M. R. J.; Clegg, W. *Organometallics* **2001**, *20*, 2533.
(25) Nöth, H.; Wrackmeyer, B. In *Nuclear Magnetic Resonance Spectroscopy of Boron Compounds*; Springer-Verlag: Berlin, 1978; pp 74−101.

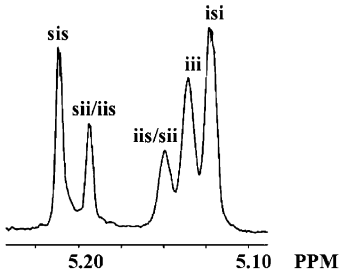

Figure 3. Homonuclear decoupled ^{1}H NMR spectrum of the methine region of hetero-biased PLA prepared from *rac*-LA with **3** at 23 °C (400 MHz, $CDCl_3$).

$CDCl_3$ is used as the polymerization medium, the resultant PLA samples show a heterotactic bias, as indicated by the enhancement in the heterotactic tetrads (sis and isi) in the spectra (Figure 3). Although the monomer conversion increased steadily with time and a linear relationship with M_n was found in $CDCl_3$, the intercept for this plot is at ca. 30 000, indicating that the catalyst deactivates quickly after the initiation. In addition, the polydispersities of the resulting polymer are broad ($PDI_{av} = 1.44$).

When the polymerization of *rac*-lactide by **3** was carried out in a 10:1 ratio, the ^{1}H NMR spectrum of the resulting oligomer revealed the presence of a methyl ester end group (δ 0.99, cf. −0.33 for the Me group in **3**). This observation indicates that the initiation of the ROP process involves nucleophilic attack by the methyl group bound to the magnesium center on the carbonyl group of *rac*-LA. Previous work with β-diketiminate {CH[(CMe)NDipp]$_2$} systems has shown this process does occur for metal−carbon bonds.[4] The resonances for the bamam-**1** ligand in the ^{1}H NMR spectrum exhibit only small shifts compared to those for the ligand in **3**. Thus the NMR data imply that the bamam ligand remains bound to the magnesium center and that the methyl group initiates polymerization. Recent studies of the polymerization of *rac*-lactide have focused on metal-alkoxy complexes.[4−7] In view of this trend and the current results for magnesium-alkyl and -aryl systems, future work with Mg-bamam complexes should be directed toward alkoxy derivatives, which will provide a more nucleophilic center than their alkyl analogues. To date, however, we have been unable to generate the desired alkoxy complexes from the reactions of **3**−**5** with alcohols.

Conclusions

Organomagnesium complexes of the type (RMgL)-bamam-**1** are obtained in good yields by treatment of the lithium derivatives (Li)bamam-**1** with Grignard reagents or (H)bamam-**1** with dibutylmagnesium**.** A combination of X-ray crystallographic and variable-temperature NMR studies shows that the transannular Mg−N interaction observed in the solid-state form of these complexes is maintained in solution. Preliminary studies of the polymerization of *rac*-lactide by solvated Mg-bamam complexes revealed that the methyl and phenyl derivatives are active initiators, whereas the isopropyl and *n*-butyl derivatives are inactive. No clear correlation between activity and the strength of the Mg−N interaction is evident. Future studies of the polymerization process will be directed toward the use of the (as yet unknown) alkoxy Mg-bamam complexes as catalysts.

(26) Bovey, F. A.; Mirau, P. A. *NMR of Polymers*; Academic Press: San Diego, 1996.

Experimental Section

Reagents and General Procedures. The compounds ^{t}BuMgCl (2.0 M solution in Et_2O), MesMgBr (1.0 M solution in Et_2O), MeMgBr (3.0 M solution in Et_2O), Bu_2Mg (1.0 M solution in heptane), PhMgCl (2.0 M solution in THF), and ^{i}PrMgCl (2.0 M solution in THF) were commercial samples (Aldrich) and used as received. The compounds (H)bamam-**1** and (Li)bamam-**1** were prepared by literature procedures.[2] *rac*-Lactide was purchased from Aldrich and was sublimed three times prior to use. Filtrations were performed using a PTFE filter disk (Acrodisc syringe filter; diameter: 25 mm; pore size: 0.45 μm). Solvents were dried with appropriate drying agents and distilled onto molecular sieves before use. All reactions and the manipulation of moisture- and/or air-sensitive products were carried out under an atmosphere of argon or under vacuum. All glassware was carefully dried prior to use.

Instrumentation. ^{1}H NMR spectra were recorded on Bruker AC 200 and DRX 400 spectrometers, and chemical shifts are reported relative to Me_4Si in $CDCl_3$. ^{11}B and ^{13}C NMR spectra were measured at 25 °C in C_6D_6 or $CDCl_3$ on a Bruker DRX 400 spectrometer using a 5 mm broadband probe (BBO probe) operating at 128.336 and 100.594 MHz, respectively. Chemical shifts are reported relative to those of $BF_3{\cdot}OEt_2$ in C_6D_6 and Me_4Si in $CDCl_3$, respectively. Line broadening parameters, used in the exponential multiplication of the free induction decays, were 50 to 0.5 Hz. Chemical shifts with a positive sign are correlated with shifts to high frequencies (downfield) of the reference compound. Elemental analyses were provided by the Analytical Services Laboratory of the Department of Chemistry, University of Calgary. Size-exclusion chromatography measurements were performed using two Styragel HT 4&2 columns (10 000 Å) calibrated with polystyrene standards and THF as the eluent at a flow rate of 1 mL/min. A refractometric detector (Waters 410 differential refractometer) was used at a temperature of 30 °C.

Preparation of (^{t}BuMg)bamam-1 (1). A solution of ^{t}BuMgCl in Et_2O (0.48 mL, 0.96 mmol) was added to a stirred solution of (Li)bamam-**1** (0.42 g, 0.87 mmol) in toluene (30 mL) at −30 °C. The reaction mixture was allowed to warm slowly to room temperature and stirred for 18 h. The pale yellow, cloudy mixture was then filtered, and the solvent was removed in vacuo. The residue was redissolved in a minimal amount of Et_2O. After concentration followed by cooling (−15 °C, 12 h), complex **1** was isolated as colorless crystals (0.37 g, 0.67 mmol, 76%). Anal. Calcd for $C_{35}H_{58}BMgN_3$: C, 75.61; H, 10.52; N, 7.56. Found: C, 75.44; H, 10.21; N, 7.90. ^{1}H NMR (C_6D_6, 25 °C): δ 7.43−6.92 (m, 8 H, Ph and aryl of Dipp), 3.77 [septet, 1 H, −C*H*(CH$_3$)$_2$, $^3J(^1H-^1H)$ = 7 Hz], 3.29 [septet, 1 H, −C*H*(CH$_3$)$_2$, $^3J(^1H-^1H)$ = 7 Hz], 2.48 (m, 2 H, −CC*H*$_2$CH$_2$CH$_2$CH$_3$), 2.32 (m, 2 H, −CCH$_2$C*H*$_2$CH$_2$CH$_3$), 1.77 (m, 2 H, −CCH$_2$CH$_2$C*H*$_2$CH$_3$), 1.52 (s, 9 H, C$_4$H$_9$), 1.46 [d, 3 H, −CH(C*H*$_3$)$_2$, $^3J(^1H-^1H)$ = 7 Hz], 1.41 [d, 3 H, −CH(C*H*$_3$)$_2$, $^3J(^1H-^1H)$ = 7 Hz], 1.27 (s, 9 H, C$_4$H$_9$), 1.20 (s, 9 H, C$_4$H$_9$), 1.12 [d, 3 H, −CH(C*H*$_3$)$_2$, $^3J(^1H-^1H)$ = 7 Hz], 0.92 [d, 3 H, −CH(C*H*$_3$)$_2$, $^3J(^1H-^1H)$ = 7 Hz], 0.71 (t, 3 H, −CCH$_2$CH$_2$CH$_2$C*H*$_3$). ^{11}B NMR (C_6D_6, 25 °C): δ 33 (br s). ^{13}C NMR (C_6D_6, 25 °C): δ 177.5 (−*C*^{n}Bu), 147.7−121.6 (Ph and aryl of Dipp), 54.8 [−*C*(CH$_3$)$_3$], 54.6 [−*C*(CH$_3$)$_3$], 35.5 [−C(*C*H$_3$)$_3$], 32.1 [−C(*C*H$_3$)$_3$], 30.9 [−C(CH$_3$)$_3$], 30.8 (−C*C*H$_2$CH$_2$CH$_2$CH$_3$), 29.2 (−CCH$_2$*C*H$_2$CH$_2$CH$_3$), 27.9 (−CCH$_2$CH$_2$*C*H$_2$CH$_3$), 26.9 [−*C*H(CH$_3$)$_2$], 25.6 [−*C*H(CH$_3$)$_2$], 24.3 [−CH(*C*H$_3$)$_2$], 23.8 [−CH(*C*H$_3$)$_2$], 23.6 [−CH(*C*H$_3$)$_2$], 16.3 [−CH(*C*H$_3$)$_2$], 15.8 (−CCH$_2$CH$_2$CH$_2$*C*H$_3$), 14.0 [Mg*C*(CH$_3$)$_3$].

Preparation of (MesMg)bamam-1 (2) and (BrMgOEt$_2$)-bamam-1. Complex **2** was prepared using the procedure described for **1** from (Li)bamam-**1** (0.16 g, 0.33 mmol) and MesMgBr in Et_2O (0.37 mL, 0.37 mmol). Complex **2** was obtained as colorless crystals (0.29 g) that cocrystallized with the complex (BrMgOEt$_2$)bamam-**1**. Anal. Calcd for $C_{75}H_{119}B_2BrMg_2N_6O$: C, 70.88; H, 9.44; N, 6.61. Found: C, 70.50; H, 9.01; N, 6.90. ^{1}H NMR (C_6D_6, 25 °C): δ 7.47−6.71 (m, 18 H, Ph, aryl of Dipp and aryl of Mes), 4.06 [septet, 1 H, −C*H*(CH$_3$)$_2$, $^3J(^1H-^1H)$ = 7 Hz], 3.78 [septet, 1 H, −C*H*(CH$_3$)$_2$, $^3J(^1H-^1H)$ = 7 Hz], 3.40 [m, 2 H, −C*H*(CH$_3$)$_2$, $^3J(^1H-^1H)$ = 7 Hz], 3.34 [m, 4 H, (CH$_3$C*H*$_2$)$_2$O], 2.56 (m, 4 H, −CC*H*$_2$CH$_2$CH$_2$CH$_3$), 2.43 [s, 6 H, −C$_6$H$_2$(C*H*$_3$)$_3$], 2.28 [s, 3 H, −C$_6$H$_2$(C*H*$_3$)$_3$], 1.99 (m, 4 H, −CCH$_2$C*H*$_2$CH$_2$CH$_3$), 1.62 [d, 6 H, −CH(C*H*$_3$)$_2$, $^3J(^1H-^1H)$ = 7 Hz], 1.45 (m, 4 H, −CCH$_2$CH$_2$C*H*$_2$CH$_3$), 1.36 [d, 6 H, −CH(C*H*$_3$)$_2$, $^3J(^1H-^1H)$ = 7 Hz], 1.32 (s, 18 H, C_4H_9), 1.23 [d, 3 H, −CH(C*H*$_3$)$_2$, $^3J(^1H-^1H)$ = 7 Hz], 1.21 (s, 18 H, C_4H_9), 1.18 [d, 6 H, −CH(C*H*$_3$)$_2$, $^3J(^1H-^1H)$ = 7 Hz], 1.15 [m, 4 H, (C*H*$_3$CH$_2$)$_2$O], 0.92 (t, 3 H, −CCH$_2$CH$_2$CH$_2$C*H*$_3$), 0.88 [d, 3 H, −CH(C*H*$_3$)$_2$, $^3J(^1H-^1H)$ = 7 Hz], 0.79 (t, 3 H, −CCH$_2$CH$_2$CH$_2$C*H*$_3$). ^{11}B NMR (C_6D_6, 25 °C): δ 34 (br s). ^{13}C NMR (C_6D_6, 25 °C): δ 178.4 (−*C*^{n}Bu), 160.0 (−*C*^{n}Bu), 147.3−122.1 (Ph, aryl of Dipp, and aryl of Mes), 65.7 [(CH$_3$*C*H$_2$)$_2$O], 56.3 [−*C*(CH$_3$)$_3$], 55.1 [−*C*(CH$_3$)$_3$], 35.8 [−C$_6$H$_2$(*C*H$_3$)$_3$], 32.7 [−C(*C*H$_3$)$_3$], 32.6 [−C$_6$H$_2$(*C*H$_3$)$_3$], 31.6 (−C*C*H$_2$CH$_2$CH$_2$CH$_3$), 29.7 (−CCH$_2$*C*H$_2$CH$_2$CH$_3$), 29.1 (−CCH$_2$CH$_2$*C*H$_2$CH$_3$), 27.9 & 27.8 [−*C*H(CH$_3$)$_2$], 26.3 [−*C*H(CH$_3$)$_2$], 24.8 [−CH(*C*H$_3$)$_2$], 24.7 [−CH(*C*H$_3$)$_2$], 24.2 [−CH(*C*H$_3$)$_2$], 23.9 [−CH(*C*H$_3$)$_2$], 21.9 [−CH(*C*H$_3$)$_2$], 14.9 [(*C*H$_3$CH$_2$)$_2$O], 14.1 (−CCH$_2$CH$_2$CH$_2$*C*H$_3$), 14.0 (−CCH$_2$CH$_2$CH$_2$*C*H$_3$).

Preparation of (MeMgOEt$_2$)bamam-1 (3). A solution of MeMgBr in Et_2O (0.36 mL, 1.08 mmol) was added to a stirred solution of (Li)bamam-**1** (0.47 g, 0.98 mmol) in toluene (30 mL) at −30 °C. The reaction mixture was allowed to warm slowly to room temperature and stirred for 18 h. The pale yellow, cloudy mixture was then filtered, and the solvent was removed in vacuo. The residue was redissolved in a minimal amount of Et_2O, subsequently removing the solvent in vacuo; this process was repeated three times. Complex **3** was isolated as a white powder (0.46 g, 0.78 mmol, 79%). Anal. Calcd for **3**·0.5(CH$_3$CH$_2$OCH$_2$CH$_3$), $C_{34}H_{57}BMgN_3O_{0.5}$: C, 74.12; H, 10.43; N, 7.63. Found: C, 73.67; H, 10.08; N, 7.81. Colorless crystals of **3** were isolated from Et_2O (−15 °C, 1 h). ^{1}H NMR (C_6D_6, 25 °C): δ 7.56−6.93 (m, 8 H, Ph and aryl of Dipp), 4.00 [septet, 1 H, −C*H*(CH$_3$)$_2$, $^3J(^1H-^1H)$ = 7 Hz], 3.24 [br m, 4 H, (CH$_3$C*H*$_2$)$_2$O], 2.54 [septet, 1 H, −C*H*(CH$_3$)$_2$, $^3J(^1H-^1H)$ = 7 Hz], 2.21 (m, 2 H, −CC*H*$_2$CH$_2$CH$_2$CH$_3$), 1.89 (m, 2 H, −CCH$_2$C*H*$_2$CH$_2$CH$_3$), 1.75 (m, 2 H, −CCH$_2$CH$_2$C*H*$_2$CH$_3$), 1.57 [d, 3 H, −CH(C*H*$_3$)$_2$, $^3J(^1H-^1H)$ = 7 Hz], 1.49 [d, 3 H, −CH(C*H*$_3$)$_2$, $^3J(^1H-^1H)$ = 7 Hz], 1.33 (s, 9 H, C_4H_9), 1.27 [d, 3 H, −CH(C*H*$_3$)$_2$, $^3J(^1H-^1H)$ = 7 Hz], 1.21 (s, 9 H, C_4H_9), 1.00 [br m, 6 H, (C*H*$_3$CH$_2$)$_2$O], 0.88 (t, 3 H, −CCH$_2$CH$_2$CH$_2$C*H*$_3$), 0.70 [d, 3 H, −CH(C*H*$_3$)$_2$, $^3J(^1H-^1H)$ = 7 Hz], −0.64 (s, 3 H, −MgC*H*$_3$). ^{11}B NMR (C_6D_6, 25 °C): δ 33 (br s). ^{13}C NMR (C_6D_6, 25 °C): δ 177.6 (−*C*^{n}Bu), 148.8−121.3 (Ph and aryl of Dipp), 65.7 [(CH$_3$*C*H$_2$)$_2$O], 55.5 [−*C*(CH$_3$)$_3$], 55.1 [−*C*(CH$_3$)$_3$], 36.6 (−*C*CH$_2$CH$_2$CH$_2$CH$_3$), 36.4 (−CCH$_2$*C*H$_2$CH$_2$CH$_3$), 32.3 [−C(*C*H$_3$)$_3$], 31.6 [−*C*H(CH$_3$)$_2$], 31.3 [−*C*H(CH$_3$)$_2$], 29.3 [−CH(*C*H$_3$)$_2$], 27.6 [−CH(*C*H$_3$)$_2$], 26.0 [−CH(*C*H$_3$)$_2$], 25.8 [−CH(*C*H$_3$)$_2$], 25.0 (−CCH$_2$CH$_2$*C*H$_2$CH$_3$), 24.4 (−CCH$_2$CH$_2$CH$_2$*C*H$_3$), 23.9 [−C(*C*H$_3$)$_3$], 15.1 [(*C*H$_3$CH$_2$)$_2$O], 14.2 (−Mg*C*H$_3$).

Preparation of (PhMgTHF)bamam-1 (4). Complex **4** was prepared using the procedure described for **1** from (Li)-bamam-**1** (0.34 g, 0.71 mmol) and PhMgCl in THF (0.39 mL, 0.78 mmol) and obtained as colorless crystals (0.26 g, 0.40 mmol, 58%). Anal. Calcd for **4**·0.5THF, $C_{43}H_{67}BMgN_3O_{1.5}$: C, 75.38; H, 9.86; N, 6.13. Found: C, 74.93; H, 9.95; N, 6.13. ^{1}H NMR (C_6D_6, 25 °C): δ 8.23−6.89 (m, 13 H, Ph and aryl of Dipp), 4.28 [septet, 1 H, −C*H*(CH$_3$)$_2$, $^3J(^1H-^1H)$ = 7 Hz], 3.36 [septet, 1 H, −C*H*(CH$_3$)$_2$, $^3J(^1H-^1H)$ = 7 Hz], 3.12 [br m, 4 H, O(C*H*$_2$)$_2$(CH$_2$)$_2$], 2.70 (m, 4 H, −CC*H*$_2$C*H*$_2$CH$_2$CH$_3$), 2.44 (m, 2 H, −CCH$_2$CH$_2$C*H*$_2$CH$_3$), 1.73 [d, 3 H, −CH(C*H*$_3$)$_2$, $^3J(^1H-^1H)$ = 7 Hz], 1.49 [d, 3 H, −CH(C*H*$_3$)$_2$, $^3J(^1H-^1H)$ = 7 Hz], 1.39 (s, 9 H, C_4H_9), 1.23 (s, 9 H, C_4H_9), 1.08 [d, 3 H, −CH(C*H*$_3$)$_2$, $^3J(^1H-^1H)$ = 7 Hz], 0.95 [br m, 4 H, O(CH$_2$)$_2$(C*H*$_2$)$_2$], 0.95 (br m, 3 H, −CCH$_2$CH$_2$CH$_2$C*H*$_3$), 0.73 [d, 3 H, −CH(C*H*$_3$)$_2$, $^3J(^1H-^1H)$ = 7 Hz]. ^{11}B NMR (C_6D_6, 25 °C): δ 33 (br s). ^{13}C NMR (C_6D_6, 25 °C): δ 177.8 (−*C*^{n}Bu), 170.0−120.2 (Ph and aryl of Dipp), 69.6 [O(*C*H$_2$)$_2$(CH$_2$)$_2$], 55.2 [−*C*(CH$_3$)$_3$], 54.2 [−*C*(CH$_3$)$_3$], 36.4 (−*C*CH$_2$CH$_2$CH$_2$CH$_3$), 31.9 [−C(*C*H$_3$)$_3$], 31.3 [−C(*C*H$_3$)$_3$], 30.2 (−CCH$_2$*C*H$_2$CH$_2$CH$_3$), 28.5 [−*C*H(CH$_3$)$_2$], 26.9 [−*C*H(CH$_3$)$_2$], 25.3 [−CH(*C*H$_3$)$_2$], 25.1 [−CH(*C*H$_3$)$_2$], 24.8 [−CH(*C*H$_3$)$_2$], 24.5 [O(CH$_2$)$_2$(*C*H$_2$)$_2$], 23.7 [−CH(*C*H$_3$)$_2$], 23.4 (−CCH$_2$CH$_2$*C*H$_2$CH$_3$), 13.8 (−CCH$_2$CH$_2$CH$_2$*C*H$_3$).

Preparation of (^{i}PrMgTHF)bamam-1 (5). Complex **5** was obtained as colorless crystals (0.27 g, 0.44 mmol, 71%) by using the procedure described for **1** from (Li)bamam-**1** (0.29 g, 0.61 mmol) and ^{i}PrMgCl in THF (0.33 mL, 0.67 mmol). Anal. Calcd for **5**·0.5THF, $C_{40}H_{69}BMgN_3O_{1.5}$: C, 73.79; H, 10.68; N, 6.45. Found: C, 73.82; H, 10.56; N, 6.64. ^{1}H NMR (C_6D_6, 25 °C): δ 7.64−6.90 (m, 8 H, Ph and aryl of Dipp), 3.91 [septet, 1 H, −C*H*(CH$_3$)$_2$, $^3J(^1H-^1H)$ = 7 Hz], 3.31 [br m, 4 H, O(C*H*$_2$)$_2$(CH$_2$)$_2$], 3.26 [septet, 1 H, −C*H*(CH$_3$)$_2$, $^3J(^1H-^1H)$ = 7 Hz], 2.58 (m, 4 H, −CC*H*$_2$C*H*$_2$CH$_2$CH$_3$), 2.30 (m, 2 H, −CCH$_2$CH$_2$C*H*$_2$CH$_3$), 1.86 [d, 6 H, −CH(C*H*$_3$)$_2$, $^3J(^1H-^1H)$ = 7 Hz], 1.62 [d, 3 H, −CH(C*H*$_3$)$_2$, $^3J(^1H-^1H)$ = 7 Hz], 1.44 [d, 3 H, −CH(C*H*$_3$)$_2$, $^3J(^1H-^1H)$ = 7 Hz], 1.35 (s, 9 H, C_4H_9), 1.24 (s, 9 H, C_4H_9), 1.15 [br m, 4 H, O(CH$_2$)$_2$(C*H*$_2$)$_2$], 1.03 [d, 3 H, −CH(C*H*$_3$)$_2$, $^3J(^1H-^1H)$ = 7 Hz], 0.91 (t, 3 H, −CCH$_2$CH$_2$CH$_2$C*H*$_3$), 0.67 [d, 3 H, −CH(C*H*$_3$)$_2$, $^3J(^1H-^1H)$ = 7 Hz], 0.46 [septet, 1 H, −C*H*(CH$_3$)$_2$, $^3J(^1H-^1H)$ = 7 Hz]. ^{11}B NMR (C_6D_6, 25 °C): δ 32 (br s). ^{13}C NMR (C_6D_6, 25 °C): δ 177.5 (−*C*^{n}Bu), 150.2−120.8 (Ph and aryl of Dipp), 69.4 [O(*C*H$_2$)$_2$(CH$_2$)$_2$], 55.3 [−*C*(CH$_3$)$_3$], 54.8 [−*C*(CH$_3$)$_3$], 36.7 (−*C*CH$_2$CH$_2$CH$_2$CH$_3$), 32.5 [−C(*C*H$_3$)$_3$], 31.9 (−CCH$_2$*C*H$_2$CH$_2$CH$_3$), 31.3 [−C(*C*H$_3$)$_3$], 29.2 (−CCH$_2$CH$_2$*C*H$_2$CH$_3$), 27.5 [−*C*H(CH$_3$)$_2$], 27.0 [−*C*H(CH$_3$)$_2$], 26.6 [−CH(*C*H$_3$)$_2$], 26.0 [−CH(*C*H$_3$)$_2$], 25.4 [−CH(*C*H$_3$)$_2$], 25.2 [O(CH$_2$)$_2$(*C*H$_2$)$_2$], 24.9 [−CH(*C*H$_3$)$_2$], 23.9 [−CH(*C*H$_3$)$_2$], 23.8 [−CH(*C*H$_3$)$_2$], 14.3 (−CCH$_2$CH$_2$CH$_2$*C*H$_3$), 10.3 [Mg*C*H(CH$_3$)$_2$].

Preparation of (^{n}BuMgOEt$_2$)bamam-1 (6). A solution of Bu$_2$Mg in heptane (1.69 mL, 1.69 mmol) was added to a stirred solution of (H)bamam-**1** (0.40 g, 0.85 mmol) in *n*-hexane (50 mL) at room temperature. The reaction mixture was stirred for 18 h, and then the solvent was removed in vacuo from the clear bright yellow mixture to give a sticky yellow residue. The residue was redissolved in a minimal amount of Et_2O. After concentration followed by cooling (−15 °C, 5 min), complex **6** was isolated as colorless crystals (0.32 g, 0.51 mmol, 60%). Anal. Calcd for **6**·0.5(CH$_3$CH$_2$OCH$_2$CH$_3$), $C_{41}H_{73}BMgN_3O_{1.5}$: C, 73.81; H, 11.03; N, 6.30. Found: C, 73.63; H, 11.08; N, 6.79. ^{1}H NMR (C_6D_6, 25 °C): δ 7.53−6.96 (m, 3 H, Ph and aryl of Dipp), 3.89 [septet, 1 H, −C*H*(CH$_3$)$_2$, $^3J(^1H-^1H)$ = 7 Hz], 3.24 [m, 1 H, −C*H*(CH$_3$)$_2$, $^3J(^1H-^1H)$ = 7 Hz], 3.24 [m, 4 H, (CH$_3$C*H*$_2$)$_2$O], 2.45 (m, 2 H, −CC*H*$_2$CH$_2$CH$_2$CH$_3$), 2.20 (m, 2 H, −CCH$_2$C*H*$_2$CH$_2$CH$_3$), 2.02 (m, 2 H, −MgCH$_2$CH$_2$C*H*$_2$CH$_3$), 1.78 (m, 2 H, −MgCH$_2$C*H*$_2$CH$_2$CH$_3$), 1.74 (m, 2 H, −CCH$_2$-CH$_2$C*H*$_2$CH$_3$), 1.52 [d, 3 H, −CH(C*H*$_3$)$_2$, $^3J(^1H-^1H)$ = 7 Hz], 1.48 [d, 3 H, −CH(C*H*$_3$)$_2$, $^3J(^1H-^1H)$ = 7 Hz], 1.26 (s, 9 H, C_4H_9), 1.21 [d, 3 H, −CH(C*H*$_3$)$_2$, $^3J(^1H-^1H)$ = 7 Hz], 1.16 (s, 9 H, C_4H_9), 1.06 [m, 6 H, (C*H*$_3$CH$_2$)$_2$O], 1.06 (m, 3 H, −MgCH$_2$-CH$_2$CH$_2$C*H*$_3$), 0.84 (t, 3 H, −CCH$_2$CH$_2$CH$_2$C*H*$_3$), 0.77 [d, 3 H, −CH(C*H*$_3$)$_2$, $^3J(^1H-^1H)$ = 7 Hz], 0.24 (m, 2 H, −MgC*H*$_2$CH$_2$-CH$_2$CH$_3$). ^{11}B NMR (C_6D_6, 25 °C): δ 33 (br s). ^{13}C NMR (C_6D_6, 25 °C): δ 176.1 (−*C*^{n}Bu), 147.6−120.7 (Ph and aryl of Dipp), 65.5 [(CH$_3$*C*H$_2$)$_2$O], 54.4 [−*C*(CH$_3$)$_3$], 54.3 [−*C*(CH$_3$)$_3$], 35.4 (−*C*CH$_2$CH$_2$CH$_2$CH$_3$), 32.8 (−MgCH$_2$*C*H$_2$CH$_2$CH$_3$), 32.1 (−MgCH$_2$CH$_2$*C*H$_2$CH$_3$), 31.6 [−C(*C*H$_3$)$_3$], 30.6 (−CCH$_2$*C*H$_2$CH$_2$-CH$_3$), 30.4 [−C(*C*H$_3$)$_3$], 28.9 [−*C*H(CH$_3$)$_2$], 27.2 [−*C*H(CH$_3$)$_2$], 25.8 [−CH(*C*H$_3$)$_2$], 25.3 [−CH(*C*H$_3$)$_2$], 23.7 [−CH(*C*H$_3$)$_2$], 23.3 [−CH(*C*H$_3$)$_2$], 23.1 (−CCH$_2$CH$_2$*C*H$_2$CH$_3$), 15.1 [(*C*H$_3$CH$_2$)$_2$O], 14.2 (−MgCH$_2$CH$_2$CH$_2$*C*H$_3$), 13.6 (−CCH$_2$CH$_2$CH$_2$*C*H$_3$), 7.5 (−Mg*C*H$_2$CH$_2$CH$_2$CH$_3$).

Table 4. Selected Crystal Data and Data Collection Parameters for 1−6[a]

	1	**2**[b]	**3**	**4**	**5**	**6**
formula	$C_{35}H_{58}BMgN_3$	$C_{75}H_{119}B_2BrMg_2N_6O$	$C_{36}H_{62}BMgN_3O$	$C_{41}H_{62}BMgN_3O$	$C_{38}H_{64}BMgN_3O$	$C_{39}H_{68}BMgN_3O$
fw	555.96	1270.91	588.01	648.06	614.04	630.08
space group	$P2_1/c$	$P\bar{1}$	$P2_1/n$	$P2_1/n$	$P2_1/n$	Cc
a, Å	9.102(1)	10.429(2)	11.099(2)	11.714(1)	10.681(2)	18.765(2)
b, Å	35.987(6)	18.902(4)	18.001(3)	20.926(2)	20.118(5)	12.116(2)
c, Å	10.833(2)	19.996(4)	18.638(3)	16.015(3)	17.836(6)	19.797(6)
α, deg	90	89.21(3)	90	90	90	90
β, deg	92.94(1)	87.62(3)	101.810(7)	95.198(5)	98.634(7)	116.952(8)
γ, deg	90	75.90(3)	90	90	90	90
V, Å^3	3543.7(1)	3819.7(1)	3644.9(1)	3909.6(9)	3789.2(2)	4012.1(1)
Z	4	2	4	4	4	4
d_{calcd}, g cm^{-3}	1.042	1.105	1.072	1.101	1.076	1.043
μ, mm^{-1}	0.076	0.598	0.079	0.079	0.078	0.075
F(000)	1224	1376	1296	1416	1352	1392
R[c]	0.065	0.045	0.052	0.047	0.063	0.042
R_w[d]	0.193	0.117	0.133	0.141	0.162	0.106

[a] Temperature = 173(2) K; wavelength = 0.71073 Å. [b] The asymmetric unit is composed of independent molecules of (MesMg)bamam-**1** and (BrMgOEt$_2$) bamam-**1**. [c] $R = \sum||F_o| - |F_c||/\sum|F_o|$ ($I > 2.00\sigma(I)$). [d] $R_w = \{[\sum w(F_o^2 - F_c^2)^2]/[\sum w(F_o^2)^2]\}^{1/2}$ (all data).

General Polymerization Procedure. *rac*-LA (0.81 g, 5.60 mmol; 0.05 g, 0.32 mmol) was dissolved in $CDCl_3$ in a vial inside an inert atmosphere glovebox. A solution of the corresponding catalyst (0.056 mmol; 0.03 mmol) in $CDCl_3$ was then added to the lactide solution ([lactide]:[catalyst] = 100:1; 10:1) in the glovebox. The reaction was stirred at room temperature for the desired period, at which time small aliquots were removed from the glovebox and the polymerization was terminated by exposure to air. Monomer conversions were determined by ^{1}H NMR analyses, and molecular weight data were acquired using size-exclusion chromatography measurements.

X-ray Analyses. Single crystals of (RMgL)bamam-**1** (colorless prism, **1**; colorless blocks, **3**, **4**, and **6**; colorless plates, **2** and **5**) were coated with Paratone 8277 oil (Exxon), mounted onto thin glass fibers, and quickly frozen in the cold nitrogen stream of the goniometer. Data were collected on a Nonius CCD four-circle Kappa FR540C diffractometer using graphite-monochromated Mo Kα radiation ($\lambda = 0.71073$ Å). Data were measured using ϕ and ω scans. Data reduction was performed by using the HKL DENZO and SCALEPACK software.[27]A multiscan absorption correction was applied to the data (SCALEPACK).[27]

Relevant parameters for the data collections and crystallographic data for (RMgL)bamam-**1** complexes **1**−**6** are summarized in Table 4. The structures were solved by direct methods (SIR-92[28]) and refined by a full-matrix least-squares method based on F^2 using SHELXL-97.[29]

The non-hydrogen atoms were refined anisotropically. Hydrogen atoms were included at geometrically idealized positions (C−H bond distances 0.95 Å) and were not refined. The final difference maps for **4** and **6** were essentially featureless with some leftover electron density in the vicinity of disordered toluene molecules. For complex **5**, THF and ^{n}Bu C atoms were disordered. The asymmetric unit of **2** is composed of independent molecules of (MesMg)bamam-**1** and (BrMgOEt$_2$)bamam-**1**.

Thermal ellipsoid plots for the crystal structures were generated using the programs CAMERON[30] and XP (part of the SHELXTL-NT 5.1[31] program library) and then imported into CorelDRAW 9.[32] Thermal ellipsoids are shown at the 30% probability level, and for clarity, H atoms are omitted and only selected carbon atoms are labeled.

Acknowledgment. We thank NSERC (Canada) for financial support, and the Alberta Ingenuity Fund and the University of Calgary for studentship awards (C.F.). We are also grateful to Jeff Hurd and Dr. G. Liu for assistance with size-exclusion chromatography measurements and Dr. M. Copsey for the X-ray structure of **2**.

Supporting Information Available: Crystallographic data in CIF format for complexes **1**−**6**. This material is available free of charge via the Internet at http://pubs.acs.org.

OM049263I

(27) HKL DENZO and SCALEPACK vl. 96: Otwinowski, Z.; Minor, W. *Processing of X-ray Diffraction Data Collected in Oscillation Mode*; Methods in Enzymology, Vol. 276: Macromolecular Crystallography, Part A.; Carter, C. W., Jr., Sweet, R. M., Eds.; Academic Press: San Diego, CA, 1997; pp 307−326.

(28) Altomare, A.; Cascarano, M.; Giacovazzo, C.; Guagliardid, A. SIR-92, A package for crystal structure solution by direct methods and refinement. *J. Appl. Crystallogr*. **1993**, *26*, 343.

(29) Sheldrick, G. M. *SHELXL 97-2*: *Program for the Solution of Crystal Structures*; University of Göttingen: Göttingen, Germany, 1997.

(30) Farrugia, L. J. WinGX v1.64.05 2003: An Integrated System of Windows Programs for the Solution, Refinement and Analysis of Single-Crystal X-ray Diffraction Data. *J. Appl. Crystallogr*. **1999**, *32*, 837.

(31) *SHELXTL-NT 5.1, XPREP, Program Library for Structure Solution and Molecular Graphics*; Bruker AXS, Inc.: Madison, WI, 1998.

(32) *CorelDRAW 9*; Corel Corporation: Ottawa, Ontario, Canada, 2000.